Journal of Biophysical Chemistry, 2016, 7, 9-29
Published Online February 2016 in SciRes. http://www.scirp.org/journal/jbpc
http://dx.doi.org/10.4236/jbpc.2016.71002

Effects of Selective Biotinylation on the Thermodynamic Stability of Human Serum Albumin

Huyen Hoang[1,2], Fidelis Manyanga[1,2,3], Moshood K. Morakinyo[1,2,4], Vincent Pinkert[1], Ferdous Sarwary[1], Daniel J. Fish[1,2,5], Greg P. Brewood[1,2], Albert S. Benight[1,2,6*]

[1]Department of Chemistry, Portland State University, Portland, USA
[2]Louisville Bioscience, Inc., Louisville, USA
[3]Department of Chemistry and Physics, Salem State University, Salem, USA
[4]Portland Technology Development, Intel Corporation, Hillsboro, USA
[5]Department of Mathematics, Portland State University, Portland, USA
[6]Department of Physics, Portland State University, Portland, USA
Email: *abenight@pdx.edu

Received 24 November 2015; accepted 1 February 2016; published 4 February 2016

Copyright © 2016 by authors and Scientific Research Publishing Inc.
This work is licensed under the Creative Commons Attribution International License (CC BY).
http://creativecommons.org/licenses/by/4.0/
Open Access

Abstract

Thermal denaturation and stability of two commercially available preparations of Human Serum Albumin (HSA), differing in their advertised level of purity, were investigated by differential scanning calorimetry (DSC). These protein samples were 99% pure HSA (termed HSA_{99}) and 96% pure HSA (termed HSA_{96}). According to the supplier, the 3% difference in purity between HSA_{96} and HSA_{99} is primarily attributed to the presence of globulins and fatty acids. Our primary aim was to investigate the utility of DSC in discerning changes in HSA that occur when the protein is specifically adducted, and determine how adduct formation manifests itself in HSA denaturation curves, or thermograms, measured by DSC. Effects of site specific covalent attachment of biotin (the adduct) on the thermodynamic stability of HSA were investigated. Each of the HSA preparations were modified by biotinylation targeting a single site, or multiple sites on the protein structure. Thermograms of both modified and unmodified HSA samples successfully demonstrated the ability of DSC to clearly discern the two HSA preparations and the presence or absence of covalent modifications. DSC thermogram analysis also provided thermodynamic characterization of the different HSA samples of the study, which provided insight into how the two forms of HSA respond to covalent modification with biotin. Consistent with published studies [1] HSA_{96}, the preparation with contaminants that contain globulins and fatty acids seems to be comprised of two forms, $HSA_{96\text{-}L}$ and $HSA_{96\text{-}H}$, with $HSA_{96\text{-}L}$ more stable than HSA_{99}. The effect of multisite biotinylation is to stabilize

*Corresponding author.

How to cite this paper: Hoang, H., Manyanga, F., Morakinyo, M.K., Pinkert, V., Sarwary, F., Fish, D.J., Brewood, G.P. and Benight, A.S. (2016) Effects of Selective Biotinylation on the Thermodynamic Stability of Human Serum Albumin. *Journal of Biophysical Chemistry*, **7**, 9-29. http://dx.doi.org/10.4236/jbpc.2016.71002

$HSA_{96\text{-}L}$ and destabilize $HSA_{96\text{-}H}$. Thermodynamic analysis suggests that the binding of ligands comprising the fatty acid and globulin-like contaminant contributes approximately 6.7 kcal/mol to the stability $HSA_{96\text{-}L}$.

Keywords

Human Serum Albumin (HSA), Differential Scanning Calorimetryl (DSC), Protein Thermodynamic Stability and Thermal Denaturation

1. Introduction

Human serum albumin (HSA) is the most prominent protein in plasma. Of the over 3000 different proteins that make up the plasma proteome, HSA has the highest relative concentration and comprises greater than 65% of the total protein by mass [2] [3]. *In vivo*, HSA plays a major role as the principal cellular transporter in blood, and in doing so binds, both reversibly and covalently, to a broad spectrum of ligands of endogenous and exogenous origins. Binding and resulting modifications can be covalent, ionic or hydrophobic in nature [4] [5]. Examinations of HSA samples derived from diseased blood have divulged a variety of chemical modifications, or adducts, of HSA that accompany human disease [6]. Levels and types of covalent modifications of HSA can vary depending on the specific disease state(s) [7].

Because of the central role it serves in biochemistry, much is known about the structure, stability and function of HSA [2]. HSA has served as a model for studies of protein folding and investigations of protein-ligand binding interactions [8]. A number of studies have investigated the structure and thermal stability of HSA [1] [9]-[16]. In these investigations a variety of spectroscopic techniques including Circular Dichroism, Infrared, and Fluorescence spectroscopy were employed. More recently (over the past 20 years) results of using Differential Scanning Calorimetry (DSC) to analyze the thermal stability of HSA have been reported [1] [9] [15] [17]-[20].

The primary structure of HSA is comprised of 585 amino acids residing on a single polypeptide chain. There are no tryptophan or methionine residues, but there is an abundance of charged residues such as lysine, arginine, glutamic acid and aspartic acid [2] [21] [22]. HSA protein monomer has a molecular weight of ~66.5 kD and its 3-dimensional structure is a heart-shaped molecule composed of three domains, each with two sub-domains denoted A and B. The structure contains 17 disulfide bridges and one free sulfhydryl on cysteine residue 34 [2]. The first 3-dimensional structure of HSA determined by X-ray crystallography was reported in 1992 [23] [24] followed by the higher resolution crystal structure [25]. These and other studies have indicated that sites for ligand binding, and particularly binding sites of fatty acids, reside in the clefts between domains of the tertiary structure where there is an abundance of charged and polar residues such as lysine and arginine [26] [27].

A primary function of HSA is to transport fatty acid (FA). Consequently, a number of studies have investigated interactions and structural consequences of FA binding to HSA. These have identified the FA binding sites and, not surprisingly, some of these are associated with lysine residues [26] [27]. Many of the same sites bound by FA are also likely targets for adduct formation or binding of other important ligands (*i.e.* therapeutic agents or diagnostic metabolites). It has been shown that FA binding can be allosteric and results in a conformational change of HSA. The FA bound conformation is apparently locked in by FA binding and conversion from the bound structure occurs with dissociation of FA [5].

Effects of FA on HSA thermodynamics were studied by one particular group [1] [15] who proposed, based on the observation of a bi-phasic thermal denaturation profile, the existence of two forms of HSA in the presence of long chain fatty acids. These were coined the defatted and un-defatted forms of HSA [1]. Since our HSA_{96} preparation also displayed a bi-phasic melting curve and contains 3% impurity specified by the supplier as “fatty acid and globulin”, the possibility that our HSA_{96} was analogous to the reported un-defatted form of HSA [1] is considered in our interpretation of the results.

In the current study our focus was on performing DSC analysis of HSA and quantitatively determining how the thermodynamic stability of HSA, an indirect measure of HSA structural integrity, is affected by covalent attachment of biotin to different sites on HSA_{99} and HSA_{96}. Through the choice of attachment chemistries, it was possible to selectively attach biotin to either a single site, or different multiple sites, and then make DSC mea-

surements to assess the effects of specific site biotinylation on HSA thermodynamic stability. Biotinylation naturally occurs in several metabolic processes and it has been previously employed as a probe of conformational changes in proteins [28]. Successful biotinylation of plasma has also been reported [29]. For these reasons site-specific biotinylation of HSA was conveniently chosen as the attachment moiety for investigating effects of covalent adduct formation on thermodynamic stability of HSA.

2. Materials and Methods

2.1. Protein Samples

Human serum albumin (HSA) was purchased from Sigma Aldrich (St. Louis, MO). Two different preparations of HSA with differing advertised purity were received as lyophilized powder. They were fatty acid and globulin free, ≥99% pure HSA (product number: A3872, lot number: SLBD740V) and ≥96% pure HSA (product number: A1653, lot number: SLBG2676V). The former was advertised as purified from the latter, but not necessarily the same batch. According to the supplier the 3% greater purity of the HSA_{99} sample is due to the absence of slight amounts of FA and globulins purified away from HSA_{96}. Hereafter, the 99%-pure and 96%-pure preparations of HSA are referred to as HSA_{99} and HSA_{96}, respectively. The latter is the well-known HSA fraction V isolated by the method of Cohn *et al*. [30]. Although fraction V yields a large relative percentage of HSA, the preparation has been shown to be contaminated by ~2% globulins, primarily α_1-globulins such as orosomucoid and long chain FA present at a Mole/Mole ratio of FA/HSA < 1. A typical value of this ratio = 0.51 was reported [2]. Although an independent analysis of the specific contaminants in our HSA_{96} preparation was not performed, the Certificate of Analysis of HSA_{96} for our lot provided by the supplier reported not more than 2% of protein contaminant (as expected for fraction V). Thus, the majority of the remaining contaminant is nominally attributed to FA. Still the overall composition of the 3% contaminant of HSA_{96} is not precisely known. To convey this fact, henceforth, the 3% impurity of HSA_{96} is referred to as the "FA- and globulin-like contaminant" (FA/G-LC), with the belief that by mass the FA/G-LC is roughly comprised of 2% globulins and not more than 1% FA. In analogy several authors reported FA-free and FA-containing HSA species that have been referred to as defatted and un-defatted HSA [1] [15] [18].

2.2. Solvents and Reagents

Standard buffer solutions contained 10 mM potassium phosphate and 150 mM NaCl, pH = 7.4. Total ionic concentrations of buffers were verified by electrical conductivity measurements. After preparation and prior to use, buffer solutions were stored at 4˚C. All solutions and buffers were prepared with Nanopure deionized water. All chemicals and reagents were molecular biology grade or higher.

2.3. Solutions of HSA

Stock solutions of HSA were prepared at 1.0 mM by dissolving 0.067 g of HSA (67 kDa) in 1 mL buffer. Generally, reconstituted protein solutions were stored at 4˚C for at least 24 hrs before use. In the case of HSA_{96}, samples that were somewhat unstable under storage were examined within 48 hrs after preparation. For DSC melting experiments, a portion of the HSA stock solution was diluted in buffer to a final concentration of 1.5 - 2.0 mg/mL.

2.4. Biotin Attachment to Multiple Sites on HSA

Biotin was attached to multiple sites on HSA by targeting the primary amines of lysine residues. Of the 59 lysine residues in the primary structure it is believed that nearly 20 of these are likely to be sufficiently exposed, and therefore accessible for covalent attachment of Biotin in the 3-D structure of HSA [26]. Biotin was attached to HSA using the EZ-Link Sulfo-NHS-Biotin kit (product number 21217 from Thermal Fisher Scientific) according to the supplier's instructions. For the attachment reactions, a 10 mM stock solution of Biotin was prepared by dissolving 3.2 mg Biotin in 500 µL of ddH_2O. A solution containing a 1:1 molar ratio of HSA:Biotin was prepared by adding 3.02 µL Biotin stock solution per mL of a HSA solution at 2 mg/mL. In this manner HSA was incubated with various amounts of Biotin at a variety of molar ratios, HSA:Biotin, up to 1:50. For these reactions appropriate amounts of the Biotin stock solutions were added to HSA in the presence of the Bio-

tin linking reagent and incubated for four hours at 20˚C. Generally, HSA samples prepared with different levels of attached Biotin were stored at 4˚C for at least 24 hours before removal of unattached free biotin. In this way Biotin was attached to both HSA_{99} and HSA_{96} preparations at a variety of HSA:Biotin ratios from 1:1 to 1:50.

2.5. Biotin Attachment to Single Sites on HSA

Biotin was covalently attached to HSA targeting the disulfides of cysteine residues. Presumably, under neutral conditions, only one reduced sulfhydryl is available for biotin attachment at cysteine-34 of the HSA structure [2], [31]. In targeting the single reduced sulfhydryl at cysteine 34 of the HSA primary structure in these reactions, biotin was assumed to attach to only a single site on HSA. In attachment reactions HSA was incubated at 21˚C for four hours in the presence of increasing amounts of attachment reagent according to instructions provided by the supplier. For these reactions the EZ-Link Maleimide-PEG2-Biotin kit (product number 21902 from Thermal Fisher Scientific) was employed according to the supplier's instructions. Sample preparations were incubated at increasing molar ratios of HSA:Biotin, from 1:1 to 1:10. Attachment reactions were performed in 4 mL at a concentration of HSA = 1.6 mg/mL in the presence of increasing amounts of attachment reagent. In this way, Biotin was attached to both HSA_{99} and HSA_{96} preparations.

2.6. Removal of Unattached Biotin

When attachment reactions were complete, free (unattached) Biotin was removed using a Zebra spin column (product #A9892 from Thermal Fisher Scientific). In this procedure, 1.5 mL of each attachment reaction solution (total volume 3 mL) was added directly to a spin column, and the sample was washed three times with 2 mL buffer. The washed sample was then retrieved and pooled.

2.7. Determination of Protein Concentrations

Protein concentrations were determined at several steps. 1) Prior to performing attachment reactions and; 2) After application of the Biotin removal kit, at each attachment ratio, prior to measuring DSC thermograms. Protein concentrations were determined using the BCA Protein Assay Kit (product #23225, Thermal Fisher Scientific).

2.8. Gel Electrophoresis

Samples were analyzed by electrophoresis on SDS polyacrylamide gels prior to, and after measurement of thermograms (not shown). Approximately 5 ug of protein sample was suspended in gel sample buffer (25 mM Tris, 192 mM glycine, 0.1% SDS, 20 mM DTT pH = 8.3) and loaded onto a BioRad Any KD™ Mini-PROTEAN®15 well gradient polyacrylamide gel. Samples were heated at 95˚C for approximately 3 minutes before loading on the gel. Gels were run in gel sample buffer until the marker lane was well separated (35 minutes); then fixed in 50% methanol, 10% glacial acetic acid solution and stained with Coomassie Blue, then de-stained in 50% methanol, 10% glacial acetic acid; further soaked in 5% acetic acid solution, removed and photographed. The gel loading buffer for the samples contained 20 mM DTT to insure samples were in a reducing environment.

2.9. DSC Measurements

All DSC melting experiments were performed using a CSC Model 6100 Nano II-Differential Scanning Calorimeter (formerly Calorimetry Sciences Corporation, Provo UT, now TA Instruments). In a DSC melting experiment the excess heat capacity, ΔC_p, is measured as a function of increasing temperature. Gasket tipped micopipettes provided an airtight means for protein/buffer injections and care was exercised in loading both buffer and sample solutions in the DSC to prevent introduction of air bubbles. The average of five buffer scans collected over the temperature range from 0 to 100˚C served as the buffer baseline for analyzing scans of protein samples. For all DSC experiments the temperature scan rate was 1˚C/min and the protein concentration was approximately 2 - 2.5 mg/ml. To prevent degassing of solutions upon heating, all measurements were made at a pressure of 3.0 atm. Following each run, before a fresh buffer and sample were loaded in the DSC, sample and

reference cells were carefully cleaned with a 95% ethanol solution.

Results of preliminary experiments (not shown) determined that the melting transition of HSA_{99} spans the temperature region between 50 and 90˚C, and this is the temperature range for all displayed thermograms. To encompass this region, the temperature range used for measuring DSC thermograms of HSA_{99} (and HSA_{96}) was from 45 and 95˚C.

2.10. DSC Data Analysis

DSC data was analyzed using the CpCalc 2.1 software package provided by the DSC manufacturer. The standard analysis procedure was comprised of six essential steps. 1) Measured heat in μW was converted to raw molar heat capacity, $\Delta C_{p\text{-}raw}(T)$ [cal/K·mol] versus temperature curves. 2) These raw curves were then normalized for protein concentration (2.0 - 2.5 mg/mL), molecular mass (66.5 kDa), partial specific volume of the protein molecules (0.733 cm^3/g) [32] and sample cell volume producing normalized $\Delta C_p(T)$ versus T curves ($\Delta C_{p\text{-}N}(T)$ versus T). 3) The measured buffer baseline scan ($\Delta C_{p\text{-}buffer}(T)$ versus T) curve was subtracted from the normalized ($\Delta C_{p\text{-}N}(T)$ versus T) sample curve producing a buffer corrected, $\Delta C_{p\text{-}buffer\ corrected}(T)$ versus T curve. 4) Next, the baseline of the buffer corrected $\Delta C_{p\text{-}buffer\ corrected}(T)$ versus T curve was determined using a polynomial function constructed by connecting the lowest and highest temperature points on the buffer corrected $\Delta C_{p\text{-}buffer\ corrected}(T)$ versus T curve (generally the range from 45˚C - 90˚C). 5) This fitted baseline was then subtracted from the $\Delta C_{p\text{-}buffer\ corrected}(T)$ versus T curve producing finally, a concentration normalized, buffer and baseline corrected $\Delta C_{p\text{-}N\text{-}buffer\text{-}baseline\text{-}corrected}(T)$ versus T curve which is the DSC melting curve, or thermogram. 6) The experimentally observed calorimetric transition enthalpy, ΔH_{cal}, was evaluated from the integrated area under the measured thermogram. The entropy, ΔS_{cal}, was evaluated from the integrated area of the $\Delta C_{p\text{-}N\text{-}buffer\text{-}baseline\text{-}corrected}(T)/T$ versus T curve. In the analyses that were performed the observed calorimetric free-energy, ΔG_{cal}, was determined using the Gibb's relationship, *i.e.*

$$\Delta G_{cal} = \Delta H_{cal} - T\Delta S_{cal}$$

The transition temperature, t_m, is the temperature of the peak height maximum on the thermogram. The t_m and evaluated measured thermodynamic parameters, $\Delta H_{cal}, \Delta S_{cal}$ and $\Delta G_{cal}(37^{\circ}\mathrm{C})$ provided quantitative characterizations of the temperature-induced melting transitions of the HSA samples. Peak heights and peak widths at half height also served as an additional means of semi-quantitative comparison of thermogram shapes.

Analysis of DSC data in this fashion was performed under the simplifying assumptions that the melting transition of HSA occurs in a two-state manner, and that the overall change in the value of ΔC_p at the initial and final temperatures is zero [33]. Other than the choice of baseline and assumption that the $\Delta C_p = 0$, no other assumptions governed evaluation of the thermodynamic transition parameters. Results indicated the impact of these assumptions was not very severe, as evaluated parameters were in reasonable agreement with published results; and relative comparisons provided quantitative insight into effects of biotinylation on HSA structure and stability. Thus, we assumed the observed evaluated parameters corresponded to the denaturation transition of the HSA species in their standard state. The standard state thermodynamic parameters evaluated from thermograms of modified and unmodified HSA_{99} and HSA_{96}, *i.e.* generally denoted, ΔH^0_{cal}, ΔS^0_{cal} and $\Delta G^0_{cal}(37^{\circ}\mathrm{C})$, were employed to interpret their observed contrasting behaviors in response to covalent attachment of biotin.

More sophisticated models that include the possibility of multi-state transitions and a non-zero ΔC_p have been applied to analyze DSC measured denaturation curves of HSA and provided evaluations of thermodynamic transition parameters [1] [13]. Obviously depending on specific features of the particular analytical model employed to analyze DSC thermograms, actual values of the thermodynamic transition parameters obtained from the analysis could differ. However, relative values of the evaluated parameters should provide a more consistent basis for comparisons of results obtained using different models for thermogram analysis.

3. Results

3.1. Melting Transitions of Unmodified HSA

The average of multiple measurements (>10) of the excess heat capacity, ΔC_p, versus temperature (thermograms) for 99% pure HSA (HSA_{99}) and 96% pure HSA (HSA_{96}) samples, are shown in **Figure 1**. The distinctly different shapes of the thermograms for HSA_{99} and HSA_{96} in **Figure 1** demonstrate the capability of DSC measure-

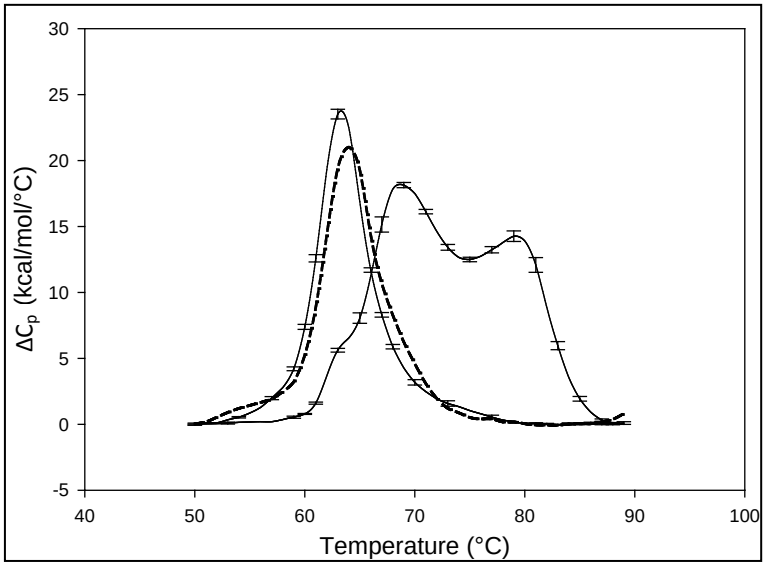

Figure 1. Thermograms for HSA_{99} and HSA_{96}. The thermogram for HSA_{99} (left curve, solid line) is single-peaked with t_m = 63.3˚C. The curve for HSA_{96} (right curve) is comprised of two overlapping major transitions with t_m's at 68.8 and 78.8˚C. Note, also a minor shoulder peak at 63.3˚C on the low temperature side of the HSA_{96} main transition. Vertical error bars depict the variations in curve shape for multiple experiments on the same sample. The t_m values vary on average 0.5˚C for multiple experiments. Thermograms of HSA_{96} and HSA_{99} (solid lines) were measured for samples prepared fresh and examined within a week of preparation. The dashed line is the thermogram for an HSA_{96} preparation that was stored for three weeks at 4˚C.

ments to discern effects on HSA of the presence of the FA- and globulin-like contaminant (FA/G-LC), advertised as comprising the 3% impurity in the case of HSA_{96}. Error bars indicate the experimental variation from the average over at least three independent experiments. The curve for HSA_{99} is the leftmost curve shown in **Figure 1**. As indicated by the error bars, in multiple DSC experiments the thermogram for HSA_{99} was highly reproducible, with a nearly symmetric melting transition, a single major peak and slight high temperature asymmetry, and average t_m = 63.3˚C ± 0.2˚C. The peak width at half height of the HSA_{99} thermogram is not more than 7˚C. The t_m and curve shape of the HSA_{99} thermogram are similar to those in published reports for defatted HSA also measured by DSC [1] [12] [17]. These reports have onset of the HSA melting transition at around 50˚C with a span of 35˚C and completed by about 85˚C. Preparations of HSA_{99} made from freshly diluted concentrated stock solutions (prepared from dry powder) and stored for over a year at 4˚C produced thermograms that were indistinguishable from those obtained from freshly prepared HSA_{99} concentrated stock solutions. Accordingly, this stability of the HSA_{99} thermogram confirms the structure of this preparation is quite stable during storage.

The average thermogram measured for HSA_{96} is also displayed in **Figure 1** (right-most curve). When the thermograms for HSA_{96}, and HSA_{99} are compared, the thermogram for HSA_{96} is shifted to higher temperature by more than 5˚C and overall the transition seems to be comprised of at least two sub-transitions centered at 68.8 and 78.8˚C. There is also a very minor peak inflection on the low temperature side of the main transition at the same temperature as the t_m of HSA_{99}. Thermodynamic transition parameters evaluated from the thermograms of HSA_{99} and HSA_{96} are summarized in **Table 1** and discussed later.

The bi-phasic melting transition observed for HSA_{96} is remarkably similar to results of published DSC melting experiments on HSA in the presence of endogenous long chain fatty acid (LCFA) [1] [15]. Measuring under nearly identical conditions (buffer and solvent, scan rate, protein concentration) these authors observed a bi-phasic melting transition attributed to coexistence of two different conformational states of HSA in the presence of LCFA. To indicate their relative affinity for binding LCFA these different forms were dubbed the "fatty acid-poor" or "defatted" and "fatty acid-rich" or "un-defatted" structures of HSA. Reportedly the bi-phasic melting transition resulted from redistribution of LCFA between the two forms, which differed in LCFA binding

Table 1. Thermodynamic transition parameters. Values for the standard state enthalpy ΔH^0, entropy ΔS^0, free-energy at 37˚C, ΔG_{37}^0, and transition temperature, t_m, measured and evaluated in DSC experiments for the samples of HSA that were prepared. Values are considered accurate to within 5%. Each transition temperature, t_m, is an average value that does not vary more than 0.5˚C in multiple experiments.

HSA_{99}	Thermodynamic parameters				HSA_{96}	Thermodynamic parameters			
	ΔH (kcal/mol)	ΔS (cal/Kmol)	ΔG_{37} (kcal/mol)	t_m (˚C)		ΔH	ΔS	ΔG_{37}	t_m
Free	163.3	488	11.9	63.3	Free	279.5	817	26.1	68.8, 78.8
M-1:1	167.2	482	17.7	68.6	M-1:1	246.1	712	25.3	72.3
M-1:3	158.6	460	15.9	69.3	M-1:3	246.3	707	27.0	76.1
M-1:10	168.8	490	16.8	67.6	M-1:10	247.8	715	26.0	73.1
Average	164.9 ± 5.5	477 ± 16	16.8 ± 0.9	68.5 ± 0.9	Average	246.7 ± 0.9	711 ± 4	26.1 ± 0.9	73.8 ± 2.0
N-1:1	196.7	580	16.8	66.1	N-1:1	274.4	809	23.5	66.2
N-1:3	186.1	544	17.4	69.1	N-1:3	246.4	723	22.2	67.8
N-1:5	193.1	561	19.1	71.1	N-1:5	245.8	720	22.5	68.2
N-1:8	198.4	570	21.6	72.6	N-1:8	248.2	722	24.3	70.1
N-1:10	196.5	567	20.7	73.3	N-1:10	251.2	735	23.2	70.3
N-1:15	205.8	590	22.8	74.8	N-1:15	237.9	690	23.9	71.8
N-1:20	204.3	586	22.6	75.3	N-1:20	233.1	674	24.1	72.5
N-1:40	203.8	586	22.1	74.8	N-1:40	217.3	626	23.2	74.3
N-1:50	235.8	684	23.7	75.1	N-1:50	219.0	630	23.6	74.7

affinity and temperature dependent stability, during the denaturation process. The observed similarity between our results and the published results [1] [15] leads to the supposition that the 3% impurity in the HSA_{96} preparation (FA/G-LC) affects HSA structure and stability in a manner similar to that reported for LCFA [1]. In support of this supposition, the reported relative amounts of LCFA present in the FA-poor (0.084 mole of LCFA per mole HSA) and FA-rich (1.43 mole LCFA per mole HSA) HSA preparations are comparable to ours and span the value of 0.51 mole of FA per mole HSA assumed for the composition of the 3% FA/G-LC in our HSA_{96} preparation.

Because of the remarkable similarity between the thermogram for HSA_{96} and published thermograms for defatted and un-defatted HSA measured under very similar solution and experimental conditions, the bi-phasic thermogram of HSA_{96} in **Figure 1** is also attributed to the presence of two protein populations. In analogy with previous reports [1] [15], and for reference in future discussions, the first peak on the HSA_{96} thermogram at 68.8˚C is designated $HSA_{96\text{-}L}$; while the second peak at 78.8˚C is referred to as $HSA_{96\text{-}H}$. The former is thought to more resemble the structure and stability of HSA_{99} (but arguably not precisely the same). This distinction is evidenced by the small shoulder peak on the low temperature side of the HSA_{96} thermogram attributed to the HSA_{99} species. This small inflection occurs precisely at the t_m of HSA_{99} (63.3˚C), and likely indicates a slight amount of HSA_{99} also present in the HSA_{96} preparation. Presumably, both $HSA_{96\text{-}L}$ and $HSA_{96\text{-}H}$ bind FA to a lesser or greater extent, respectively [16]. Similarity of the melting characteristics of the HSA_{99} and HSA_{96} preparations with published results also provided assurance of the fidelity and initial native state of these HSA preparations prior to covalent attachment of biotin. Before describing results of experiments on biotinylated HSA_{99} and HSA_{96}, several additional aspects of their behavior are described.

3.2. The Labile State of HSA_{96} and Conversion of HSA_{96} to HSA_{99}

The HSA_{96} preparation was not as stable in storage as HSA_{99}. Examination of the HSA_{96} thermograms at different times after preparation indicated the average HSA_{96} thermogram displayed in **Figure 1** was reproducible for

at least one week (but not for much longer). On multiple occasions over the course of this study we observed the HSA_{96} thermogram was not always reproducible for samples stored at 4˚C for longer than a week.

According to their thermograms, spontaneous conversion of HSA_{96} to HSA_{99} was observed. Accepting that HSA_{96} contains a mixture of $HSA_{96\text{-}L}$ and $HSA_{96\text{-}H}$ the thermograms of HSA_{96} (**Figure 1**) were found to differ for different preparations, and in particular to be quite sensitive to age of the sample (after those preparations) when the thermograms were measured. With this lability of the HSA_{96} samples, reported thermograms for HSA_{96} (displayed in **Figure 1**) were obtained for protein samples that were made from HSA_{96} stock solutions prepared fresh from powder and examined within (at most) one week following preparation. Generally the time after preparation when thermograms were measured for HSA_{96} and its biotinylated derivatives was 24 to 72 hours.

Although a systematic study of the state of the HSA_{96} preparation at different times after preparation was not performed, typical results are shown in **Figure 1**. There, the thermogram of HSA_{99} (freshly prepared and less than a week old, solid line) is compared with that obtained for a preparation of HSA_{96} stored for three weeks prior to examination by DSC (dotted line). Clearly, the thermogram for the older HSA_{96} is very similar to that of HSA_{99}, evidencing conversion. Such conversion was observed in as little as one week for some HSA_{96} samples stored at 4˚C.

Experiments investigating the reversibility of the HSA_{99} melting transition were also performed (data not shown). For this investigation thermograms were measured for HSA_{99} samples first heated in separate experiments to temperatures from 30 to 70˚C, cooled at the same rate, and then re-heated from 20 to 100˚C. Results showed when HSA_{99} was first heated to temperatures up to 60˚C, just at the edge of the melting transition, cooled and re-melted, the thermogram was not different from the thermogram of unheated HSA_{99}; with a single peak, t_m = 63.3˚C. This result was taken to indicate that up to about 60˚C, corresponding to early onset of the melting transition, the measured thermogram was unaffected by prior heating and cooling, and was reversible. In contrast, when the HSA_{99} solution was pre-heated to temperatures above t_m, *i.e.* up to 80˚C, cooled and re-melted, the observed thermograms for the pre-heated samples were very different from those observed for the unheated (or reversible) curves. These results were in concordance with those reported in published studies of HSA, that HSA melting is reversible up to ≈62˚C [12] [13]. From experiments performed under conditions similar to ours these same authors found at temperatures above 75˚C, HSA resides in an irreversibly denatured, predominantly molten globule state. Reportedly, the rate of the irreversible reaction was considerably slower at lower temperatures (below 74˚C) [12]. Under experimental conditions comparable to ours these authors asserted that even up to 74˚C the denaturation reaction is predominantly reversible. This is a major operating assumption.

3.3. Melting Transitions of HSA with Biotin Covalently Attached at a Single Site

Figure 2 shows the thermograms for HSA_{99} and HSA_{96} modified by biotinylation at a single site. Protein samples that produced the results shown in **Figure 2** were prepared by using the Maleimide-activated reagent targeting the single reduced sufhydryl at cys-35 of the HSA primary structure. Products of the reactions were either HSA_{99} or HSA_{96} with biotin attached, denoted $HSA_{99\text{-}M(x:1)}$ or $HSA_{96\text{-}M(x:1)}$, respectively (M = biotin attached with Maleimide). In **Figure 2**, thermograms are displayed for $HSA_{99\text{-}M(x:1)}$ (a) or $HSA_{96\text{-}M(x:1)}$ (b) incubated at molar ratios of biotin:HSA_{99} = 1:1, 3:1 and 10:1 (x = 1, 3, 10). Error bars show experimental variation from the average curve (symbols) for $HSA_{99\text{-}M(x:1)}$ at each incubation ratio. As seen in **Figure 2(a)**, the effect of attachment on the HSA_{99} thermogram is a peak height reduced by nearly 40% and shift of t_m upward in temperature by over 5˚C. At x = 1 the peak width at half height increases by more than a factor of two. After these most dramatic changes initially at a 1:1 ratio, thermograms measured at biotinylation ratios of x = 3 and x = 10 are not greatly different. They have essentially the same t_m with only slight increases in peak widths on the high temperature side; and peak heights are the same (within error). Results of these changes associated with biotin attachment also manifest in the measured thermodynamic parameters for $HSA_{99\text{-}M(x:1)}$ summarized in **Table 1**. The evaluated parameters, t_m, $\Delta H^0_{cal}, \Delta S^0_{cal}$ and ΔG^0_{cal} for $HSA_{99:M(x:1)}$ show little variation between the different biotinylation ratios of x = 1, 3, 10.

In the same manner as for HSA_{99}, biotin was covalently attached to HSA_{96} (prepared fresh) and the thermograms were measured within 48 hours of sample preparation. Thermograms collected for the covalently modified HSA_{96} are shown in **Figure 2(b)**, and denoted $HSA_{96\text{-}M(x:1)}$. Effects of single site attachment of biotin to HSA_{96} are dramatic, and there is a very clear difference between the HSA_{96} thermogram and the $HSA_{96\text{-}M(x:1)}$

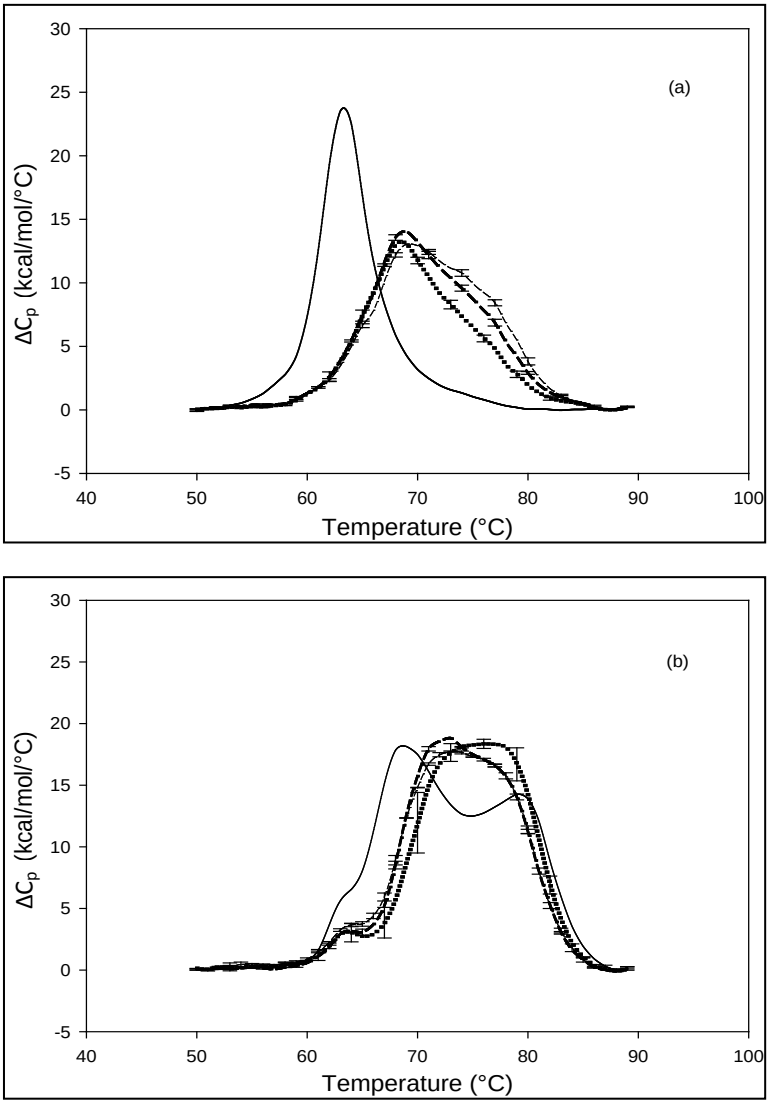

Figure 2. Thermograms of HSA modified by biotinylation at a single site. Samples were prepared as described in the text using the Maleimide-activated reagent. (a) Thermograms for HSA_{99} (solid line) and samples of HSA_{99} with biotin attached denoted $HSA_{99\text{-}M(x:1)}$. Curves shown are for the $HSA_{99\text{-}M(x:1)}$ samples prepared at attachment ratios of x = 1 (bold dash line), x = 3 (dotted line) and x = 10 (light dashed line). (b) Thermograms for HSA_{96} (solid line) and HSA_{96} with biotin attached, termed $HSA_{96\text{-}M(x:1)}$. Curves shown are for attachment ratios of x =1 (bold dash line), x = 3 (dotted line), and x = 10 (dash line).

thermograms. Responses to biotin attachment at a single site on HSA_{96} might be unexpected for several reasons. 1) As indicated by the bi-phasic thermogram in **Figure 1**, the preparation of HSA_{96} is comprised of two different forms that have been denoted $HSA_{96\text{-}H}$ and $HSA_{96\text{-}L}$, present in their respective mole fractions. 2) The effect of the biotinylation reaction on the relative population of these two states of HSA is unknown. 3) The bi-phasic nature of the HSA_{96} thermogram indicates $HSA_{96\text{-}H}$ is more stable against denaturation than $HSA_{96\text{-}L}$.

Presumably, when the attachment reaction is performed using HSA_{96}, both components, $HSA_{96\text{-}H}$ and $HSA_{96\text{-}L}$ are targeted for biotinylation. At incubation ratios of $x \geq 1$, the two-peaked thermogram of HSA_{96} in **Figure 1** with t_m's at 68.8 and 78.8˚C is consolidated into a broad, single-peaked transition with an intermediate t_m = 72.3˚C. The peak height is roughly the same as the major peak at 68.8˚C on the thermogram of HSA_{96} alone (solid line).

Consolidation of the thermogram in **Figure 2(b)** seems to arise from a shift up in temperature of the major peak attributed to labeled $HSA_{96\text{-}L}$ ($HSA_{96\text{-}L\text{-}M(1:1)}$). The higher temperature peak corresponding to labeled $HSA_{96\text{-}H}$ ($HSA_{96\text{-}H\text{-}M(1:1)}$) seems to have shifted down a few degrees and become absorbed into the consolidated peak brought about by the up-shifted $HSA_{96\text{-}L\text{-}M(1:1)}$ peak. The peak widths at half height of the thermograms for the $HSA_{96\text{-}M(x:1)}$ samples in **Figure 2(b)** are reduced from that of HSA_{96} (~20˚) to approximately 15˚C. Again as expected for a single biotinylation site, once saturation occurs (at x =1) incubation at increased ratios of biotin has little effect on the thermogram shape, or t_m. In effect, there are no significant differences in the thermograms for $HSA_{96\text{-}M(x:1)}$ at $x \geq 1$. Just as observed for $HSA_{99\text{-}M(x:1)}$ thermodynamic transition parameters for $HSA_{96\text{-}M(x:1)}$ summarized in **Table 1** are essentially the same at all attachment ratios examined. Although they show a similar response to biotinylation the actual thermograms of $HSA_{99\text{-}M(x:1)}$ and $HSA_{96\text{-}M(x:1)}$ are different. The peaks of the $HSA_{99\text{-}M}$ thermograms are sharper with an average t_m = 68.5˚C compared to the broader symmetric peaks of the $HSA_{96\text{-}M(x:1)}$ thermograms with average t_m = 73.8˚C. As shown in **Table 1**, and discussed in detail later, evaluated thermodynamic parameters for the thermograms of $HSA_{96\text{-}M(x:1)}$ and $HSA_{99\text{-}M(x:1)}$ also displayed different responses to biotin attachment.

3.4. Melting Transitions of HSA with Biotin Covalently Attached at Multiple Sites

The primary structure of HSA contains 59 lysine residues. Examination of the HSA crystal structure and results of cross linking studies suggested nearly half of the 59 lysine residues in HSA could be adequately exposed and therefore presumably accessible for biotinylation [26] [27]. HSA samples that produced the thermograms shown in **Figure 3** and **Figure 4** were prepared by using the NHS-activated biotin reagent targeting the primary amines of lysine residues for attachment with increasing amounts of biotin. Thermograms of NHS biotinylated HSA_{99}, denoted $HSA_{99\text{-}NS(x:1)}$, are shown in **Figure 3**. NS corresponds to biotin attached with NHS. Different thermograms shown in **Figure 3** are for samples with increasing amounts of attached biotin.

Thermograms in **Figure 3(a)** are for $HSA_{99:NS(x:1)}$ samples where the attachment ratios varied from x = 1 to 10. **Figure 3(b)** shows the thermograms obtained for $HSA_{99:NS(x:1)}$ samples for which the incubation ratio varied from x = 10 to 50. Differences in the thermograms of $HSA_{99\text{-}NS(x:1)}$ and HSA_{99} seen in **Figure 3** indicate a very clear effect of biotinylation. With increased attachment ratios from x = 1 to 20 there is a corresponding shift of the thermograms to higher temperature with incrementally increased t_m. The peak heights of the modified thermograms are all about the same and reduced by about 15% from that of HSA_{99}. Peak widths at half height of the modified thermograms increase by nearly 50% from the thermogram of HSA_{99} alone. **Figure 3(b)** shows the thermograms obtained for $HSA_{99\text{-}NS(x:1)}$ at incubation ratios from x = 10 to 50. Up to x = 20, the thermogram t_m is shifted up in a titratable fashion by more than 9˚C. At higher incubation ratios examined (x = 40, 50) there are no further changes in t_m. At incubation ratios greater than x = 10, the peak heights and widths at half height vary somewhat. Even with this variation, evaluated thermodynamic parameters in **Table 1** are very consistent.

Thermograms of HSA_{96} biotinylated at multiple sites are shown in **Figure 4**, and denoted $HSA_{96\text{-}NS(x:1)}$ where again x is the incubation ratio corresponding to the relative amount of biotin attachment. Thermograms were measured for x = 1, 3, 5, 8, 10, 15, 20, 40, 50. A sampling of these is shown in **Figure 4**. Thermograms shown in **Figure 4(a)** were measured for $HSA_{96\text{-}NS(x:1)}$ samples prepared at incubation ratios varying from x = 1 to 10. Thermograms in **Figure 4(b)** were obtained for $HSA_{96\text{-}NS(x:1)}$ samples prepared at higher incubation ratios from x = 10 to 50. There is a stark difference between the HSA_{96} thermogram (thin black line) and the $HSA_{96\text{-}NS(x:1)}$ thermograms. Most notably, at the lowest attachment ratio (x = 1) the formerly two-peaked HSA_{96} thermogram (thin black line in **Figure 4(a)**) becomes single peaked with t_m = 66.2˚C (bold dash line **Figure 4(a)**). For $x \geq 1$ the $HSA_{96\text{-}NS(x:1)}$ thermograms have the same shape but are shifted up in temperature, with increased t_m at higher attachment ratios up to about x = 40, with no changes thereafter (**Figure 4(b)**).

It is important to recall and consider that the initial preparation of HSA_{96} from which the $HSA_{96\text{-}NS(x:1)}$ samples were prepared was comprised of a mixture of two forms of HSA (referred to earlier as $HSA_{96\text{-}H}$ and $HSA_{96\text{-}L}$). Accordingly as seen in **Figure 4** for HSA_{96} the effect of biotinylation at lysine residues is different from that for single site biotinylation at cys-35 (**Figure 2(b)**). On the thermograms of $HSA_{96:NS(x:1)}$ (**Figure 4**) there is no sign of the high temperature transition at 78.8˚C, denoted $HSA_{96\text{-}H}$, suggesting the attachment reaction itself must result in conversion of the originally present more stable structure, to a less stable one. The converted less stable form, $HSA_{96\text{-}L}$, when modified at a 1:1 ratio becomes $HSA_{96\text{-}NS(1:1)}$ which is quite qualitatively similar to $HSA_{99\text{-}NS(1:1)}$, with an identical t_m. Similar comparisons can also be made between $HSA_{96\text{-}NS(x:1)}$ and $HSA_{99\text{-}NS(x:1)}$ at increasing values of x (discussed later).

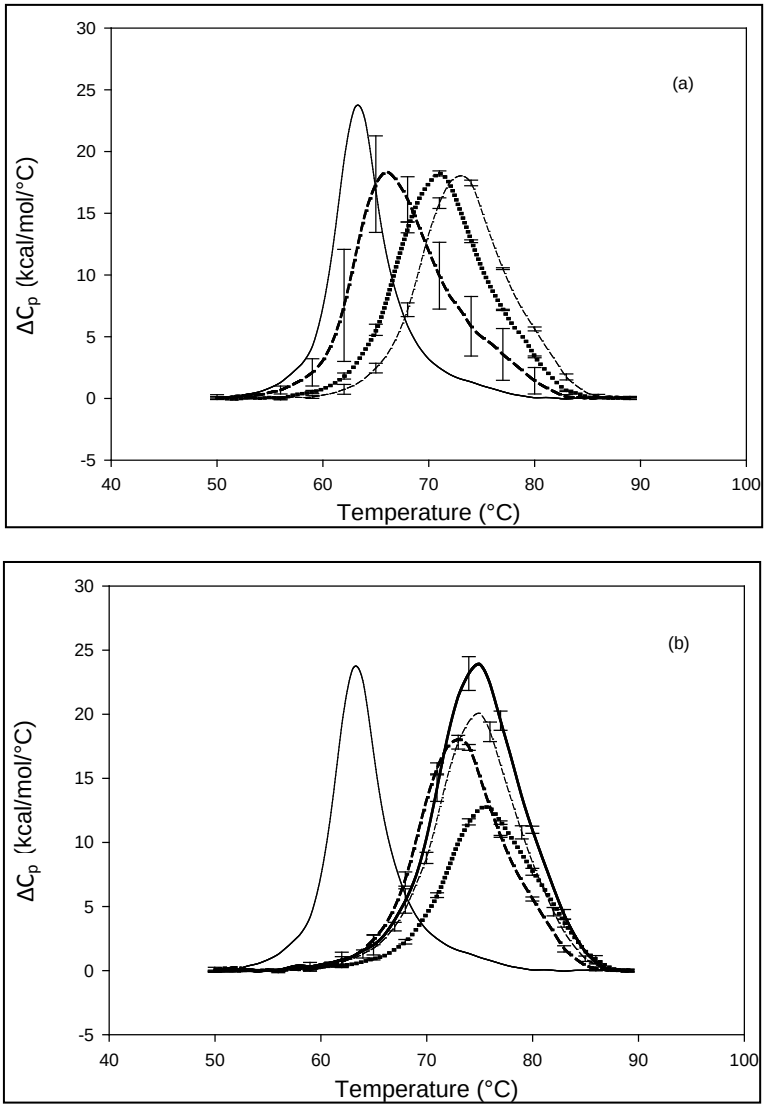

Figure 3. Thermograms for HSA_{99} modified by biotinylation at multiple sites using the NHS-activated biotin reagent as described in the text. Samples of the NHS biotinylated HSA_{99} are denoted $HSA_{99\text{-}NS(x:1)}$. (a) Thermograms for $HSA_{99:NS(x:1)}$ samples, for attachment ratios, x = 1 (bold dash line), x = 3 (dotted line), x = 10 (thin dashed line). (b) Thermograms for $HSA_{99\text{-}NS(x:1)}$ samples at incubation ratios x = 10 (thick dashed line), x = 20 (dottedline), x = 40 (thin dash line) and x = 50 (thick solid line). For comparison the thin solid line in (a) and (b) is the HSA_{99} thermogram reproduced from **Figure 1**.

Thermograms of HSA_{96} samples incubated under the same conditions as the attachment reactions (four hours at 21˚C), without the attachment reagents, were indistinguishable from the thermogram of freshly prepared HSA_{96} samples (not shown).

In summary, results in **Figure 1** through **Figure 4** clearly demonstrate the ability of DSC thermograms of HSA to detect the presence or absence of a slight amount of contaminant that contains globulins and FA, denoted earlier as FA/G-LC (**Figure 1**); detect changing states of HSA samples over time (**Figure 1**); differentiate covalent modification of HSA at a single site (**Figure 2**); or at multiple sites (**Figure 3** and **Figure 4**). For both species of HSA, the effect of single site modification is a thermogram reduced in peak height with a small shift up in t_m. For multiple site modification the thermogram displays a significant temperature shift up with increasing amounts of biotinylation.

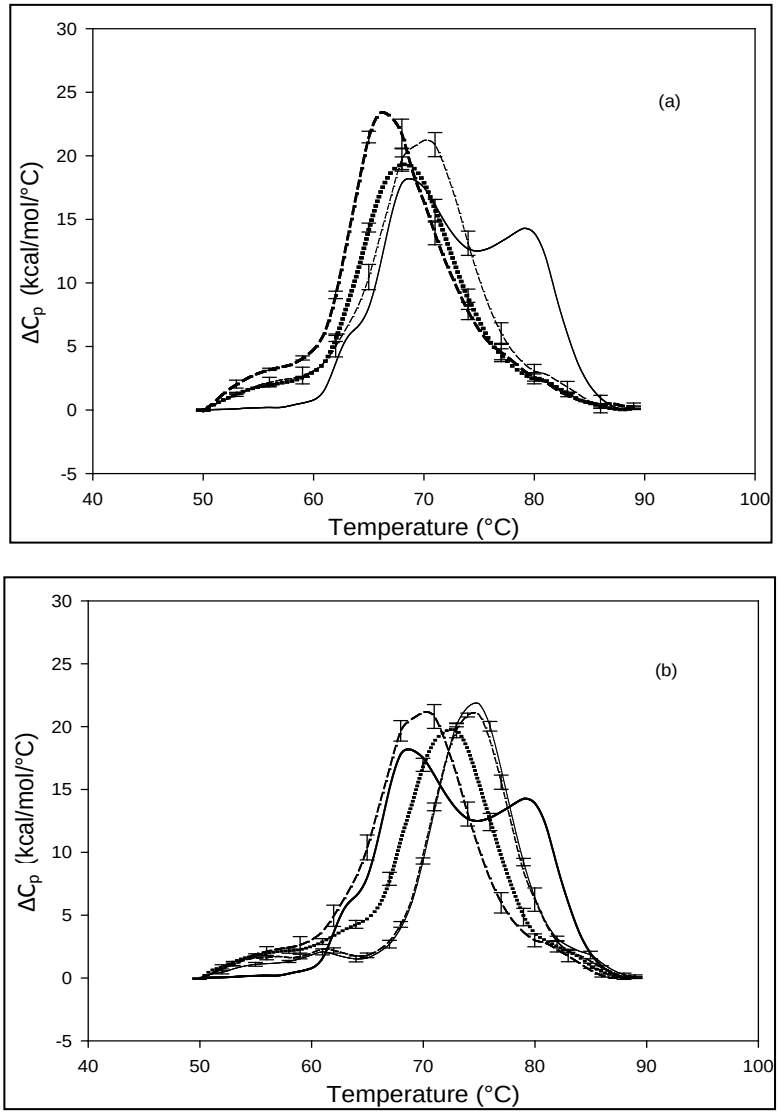

Figure 4. Thermograms for HSA_{96} biotinylated at multiple sites, denoted $HSA_{96\text{-}NS(x:1)}$, are shown at different attachment ratios, x (a) Thermograms measured for $HSA_{96\text{-}NS(x:1)}$ samples prepared at incubation ratios of x = 1 (bold dash line); x = 5 (dotted line); x = 10 (thin dash line). (b) Thermograms measured for $HSA_{96\text{-}NS(x:1)}$ samples prepared at higher incubation ratios from x = 10 (bold dash line); x = 15 (dotted line), x = 40 (thin dash line); x = 50 (thin solid line).

3.5. Thermodynamic Transition Parameters

DSC measurements provided evaluations of the thermodynamic parameters of HSA melting transitions. The enthalpy, ΔH^0_{cal}, entropy, ΔS^0_{cal}, and standard state free-energy at 37˚C, ΔG^0_{37}, and corresponding t_m's of the melting transitions of the different HSA samples of this study are summarized in **Table 1**. Comparison of the evaluated thermodynamic parameters in **Table 1** reveals differences between $HSA_{96\text{-}NS(x:1)}$ and $HSA_{99\text{-}NS(x:1)}$. Differences between the two samples at lower attachment ratios up to x = 20 suggest the $HSA_{96\text{-}L\text{-}NS(x:1)}$ samples at the lower attachment ratios reside in a different state than that of $HSA_{99\text{-}NS(x:1)}$. That is, $HSA_{96\text{-}L\text{-}NS(x:1)}$ can also be bound by components of the FA/G-LC contaminant present in the HSA_{96} preparation. The measured t_m's of $HSA_{96\text{-}NS(x:1)}$ are plotted versus attachment ratio, x, in **Figure 5** (open symbols) and compared with the behavior of $HSA_{99\text{-}NS(x:1)}$ (filled symbols). At lower attachment ratios, $HSA_{96:NS(x:1)}$ is actually less stable than $HSA_{99\text{-}NS(x:1)}$, indicating the proposed $HSA_{96\text{-}L\text{-}NS(x:1)}$ structure (with the presence of FA-containing ligands) is less stable than

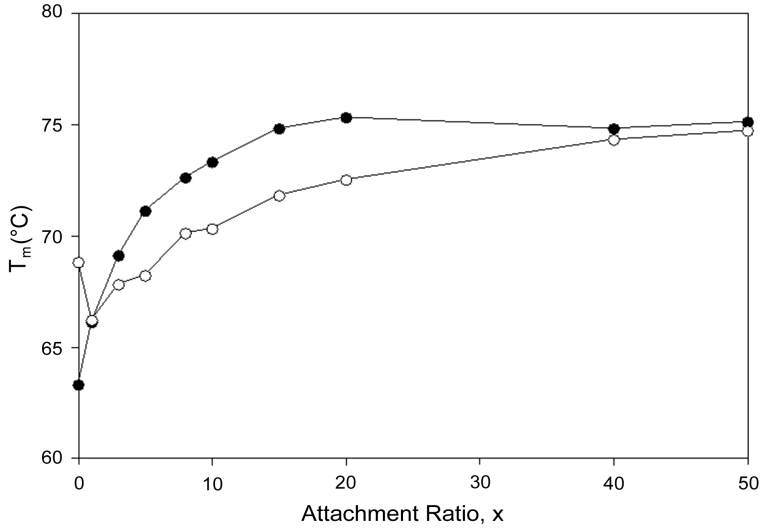

Figure 5. t_m versus attachment ratio for $HSA_{96\text{-}NS(x:1)}$ (open symbols) and $HSA_{99\text{-}NS(x:1)}$ (filled symbols). For $HSA_{96\text{-}NS(x:1)}$ t_m also approaches 75˚C at higher x values, but does so more slowly than $HSA_{99\text{-}NS(x:1)}$.

its $HSA_{99\text{-}NS(x:1)}$ counterparts at the same values of x. At higher incubation ratios (≥1:20) t_m's of the thermograms level off to around 75˚C.

Figure 5 shows for $HSA_{96\text{-}NS(x:1)}$ that t_m also approaches 75˚C at higher x values, but does so more slowly than $HSA_{99\text{-}NS(X:1)}$. In **Figure 5** the t_m's of the $HSA_{99\text{-}NS(1:x)}$ preparation (at least for $x \leq 20$) indicate it is apparently more stable against thermal denaturation than $HSA_{96\text{-}L\text{-}NS(1:x)}$ at the same x. The thermodynamic parameters evaluated for $HSA_{96:NS(x:1)}$ and $HSA_{99:NS(x:1)}$ (ΔH^0_{cal} and ΔS^0_{cal}) versus x displayed the same qualitative behavior as displayed for ΔG^0_{37} versus x in **Figure 6** (not shown). For comparisons that follow values of t_m and ΔG^0_{37} versus x are utilized. Observed trends in t_m and ΔG^0_{37} with covalent attachment of biotin to HSA_{99} and HSA_{96} provide an indication of the effects of biotinylation on thermodynamic stability. As shown in **Figure 5** and **Figure 6**, these parameters show very different responses of the two HSA forms to covalent modification by biotin. In **Figure 6** the ΔG^0_{37} values from **Table 1** are plotted versus attachment ratio for the $HSA_{99\text{-}NS(x:1)}$ and $HSA_{96\text{-}NS(x:1)}$ preparations. This plot reveals differences at the lowest attachment ratios, the plots reaching near equivalence around x = 15. Interestingly, ΔG^0_{37} is greater for the $HSA_{96\text{-}NS(1:x)}$ preparation, even though the t_m is lower than that for $HSA_{99\text{-}NS(x:1)}$ at comparable x. This observation could be due to effects of irreversible aggregation in the denaturation region.

HSA_{99} (without the FA/G-LC contaminant) aggregates more readily in the denaturation region, *i.e.* has a higher rate of intermolecular aggregation mediated by the melted state than the populations of $HSA_{96\text{-}H}$ and $HSA_{96\text{-}L}$ that comprise the HSA_{96} preparation [1]. FA is known to mediate aggregation in the denaturation region, thus the greater stability of $HSA_{96\text{-}H}$. By the same argument, attachment of biotin to HSA_{99} to form $HSA_{99\text{-}NS(1:x)}$ must also act to decrease irreversible aggregation, as the stability of $HSA_{99\text{-}NS(1:x)}$ is increased by more attachment. Then **Figure 6** suggests irreversible aggregation in the denaturation region is increasingly discouraged by increased amounts of biotinylation. The result is values of ΔG^0_{37} for $HSA_{99\text{-}NS(x:1)}$ that are smaller than for $HSA_{96\text{-}NS(x:1)}$ at the lower attachment ratios (as plotted in **Figure 6**), but equivalent at higher ratios.

Prior to comparison, discussion and interpretation of tabulated thermodynamic parameters it should be noted that parameter evaluations were made under the assumption that HSA melting from the native to the denatured state predominantly occurs in a two-state manner. Several published studies have reported results of measurements on HSA and thermodynamic transition parameters of the HSA melting transition [1] [13] [17]. In these reports different methods of data analysis, baseline treatment, model assumptions and curve fitting were employed. Ours is a standard approach, and arguably one of the least sophisticated that has been applied, with several simplifying assumptions. As discussed below relative comparisons of the parameters within the data set were considered to be quantitatively significant, and provided additional insight into the consequences of biotin attachment on the different HSA samples. Melting transition parameters evaluated by DSC analysis of HSA_{99},

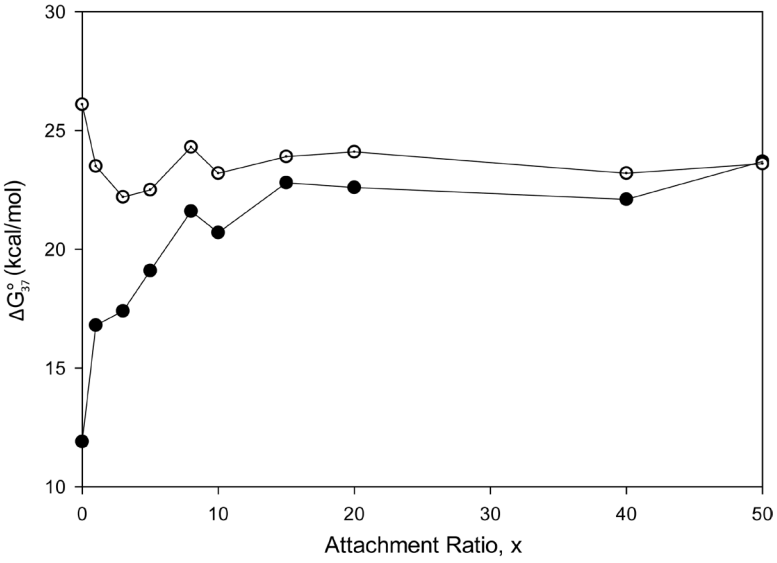

Figure 6. ΔG^0_{37} values from **Table 1** plotted versus attachment ratio, *x*, for the $HSA_{99\text{-}NS(x:1)}$ (filled symbols) and $HSA_{96\text{-}NS(x:1)}$ preparations (open symbols).

HSA_{96} and their modified versions with biotin attached, $HSA_{99\text{-}M(x:1)}$, $HSA_{99\text{-}NS(x:1)}$, $HSA_{96\text{-}M(x:1)}$ and $HSA_{96\text{-}NS(x:1)}$ are summarized in **Table 1**.

A few general features of the parameter sets are noteworthy. 1) For both preparations of unmodified HSA alone, HSA_{99} and HSA_{96} measured values (ΔH^0_{cal} = 163.3 kcal/mole for HSA_{99}), (ΔH^0_{cal} = 279.5 kcal/mole for HSA_{96}) approach, or are within, the range of reported values for defatted and un-defatted HSA [1] [13] [17]. This general agreement indicates our simplifying assumptions of a two-state melting transition with $\Delta C_p = 0$, and variations in baseline analysis procedures must have a small effect on the quantitative significance of the evaluated thermodynamic parameters. 2) Response of the t_m of HSA to covalent attachment of biotin is different for HSA_{99} than for HSA_{96}. For $HSA_{99\text{-}M(x:1)}$ at (x = 1), the t_m increases by over 5˚C, and does not change further at higher attachment ratios. The average (over all attachment ratios) is t_m = 68.7 ± 0.4˚C. Response of the thermodynamic parameters ΔH^0_{cal}, ΔS^0_{cal} and ΔG^0_{37} for $HSA_{99\text{-}M(x:1)}$ concurs with that for the t_m. For $HSA_{99\text{-}M(x:1)}$ ΔG^0_{37} increases to the same value at ratios of x = 1, 3 and 10 with an average value of 16.8 ± 0.9 kcal/mol. In contrast, under the same conditions for $HSA_{96\text{-}M(x:1)}$ samples at attachment ratios of x = 1, 3 and 10 there is a nearly 13% decrease in ΔH^0_{cal} and ΔS^0_{cal} values, but ΔG^0_{37} values for modified $HSA_{96\text{-}M(x:1)}$ are identical to that of unmodified HSA_{96} with average ΔG^0_{37} = 26.1 ± 0.9 kcal/mol. To summarize for the cases of $HSA_{99\text{-}M(x:1)}$ and $HSA_{96\text{-}M(x:1)}$, both show no difference between the attachment ratios (x = 1, 3, 10), consistent with single site attachment. For $HSA_{99\text{-}M(x:1)}$ biotin attachment results in an increase in stability (ΔG^0_{37}) while $HSA_{96\text{-}M(x:1)}$ displays the same stability as HSA_{96}.

In contrast, opposite responses of ΔH^0_{cal} and ΔS^0_{cal}, and in particular ΔG^0_{37}, to attachment of biotin to amines of lysine residues were found for $HSA_{99\text{-}NS(x:1)}$ compared to $HSA_{96\text{-}NS(x:1)}$. For $HSA_{99\text{-}NS(x:1)}$ the t_m increases incrementally with increasing attachment ratios x > 20 for a total increase of nearly 10˚C, and levels off thereafter (see **Figure 5**). Examination of **Table 1** indicates the thermodynamic parameters for $HSA_{99\text{-}NS(x:1)}$ and $HSA_{96\text{-}NS(x:1)}$ tend in opposite directions. In comparison consider the behavior of ΔG^0_{37} values versus attachment ratio as plotted in **Figure 6**. As shown there, for $HSA_{99\text{-}NS(x:1)}$ at x = 1, ΔG^0_{37} *increases* and continues to do so in an incremental fashion up to an attachment ratio of x = 15 where after it levels off and is constant up to the highest ratios (x = 40, 50). In contrast for $HSA_{96\text{-}NS(x:1)}$, at an attachment ratio of x =1, ΔG^0_{37} decreases from the value for HSA_{96} and decreases again for x = 3 and 5; dramatically increases at x = 8, then levels off at the higher ratios (see **Figure 6**). The opposite responses of the ΔG^0_{37} values for $HSA_{99\text{-}NS(x:1)}$ and $HSA_{96\text{-}NS(x:1)}$ as a function of increased attachment ratio reveals an effect of the presence of the small amount (3%) of FA/G-LC on modified HSA. The contrasting observations are: 1) Attachment *increases* stability (ΔG^0_{37}) of the $HSA_{99\text{-}NS(x:1)}$ samples compared to HSA_{99} alone. This stability enhancement occurs in an incremental fashion up to 1:15 were presumably saturation of available attachment sites is reached. 2) Attachment dramatically *decreases* stability

(ΔG^0_{37}) of the $HSA_{96\text{-}NS(x:1)}$ samples at the lowest attachment ratios (x = 1 - 10); thereafter at increased attachment ratios ($x \geq 10$) ΔG^0_{37} converges to a constant value of higher stability, but with less stability than HSA_{96} alone.

4. Discussion

4.1. Thermodynamic Interpretation of Results

In order to provide an interpretation of the thermodynamic measurements of the two forms of HSA and consequences of biotinylation of them, consider the following simple model of thermal denaturation of HSA written as the following reaction,

$$HSA_N \underset{}{\overset{K^0_{obs}}{\rightleftharpoons}} HSA_D \tag{1}$$

where the transition is assumed to occur in a pseudo two-state manner from the native intact structure, HSA_N, to the denatured state, HSA_D. This reaction occurs with an observed standard state equilibrium constant, K^0_{obs}. The observed standard state free-energy is given by $\Delta G^0_{obs} = -RT \ln K^0_{obs}$. At temperatures below t_m the standard state free-energy, $\Delta G^0_{obs} > 0$ and the native structure is favored.

The equilibrium reaction in Equation (1) can be represented in terms of the corresponding chemical potentials as,

$$\mu^0_N \rightleftharpoons \mu^0_D \tag{2}$$

where μ^0_N and μ^0_D are the hypothetical standard state chemical potentials for the native state (N) and the denatured state (D), respectively. The standard state free energy, ΔG^0_{obs}, is given in terms of the differences of the standard state chemical potentials of the native and denatured states, *i.e.*

$$\Delta G^0_{obs} = \mu^0_D - \mu^0_N \tag{3}$$

The observed standard state equilibrium constant for the reaction is also given by,

$$K^0_{obs} = \frac{X_D}{X_N} = \mathrm{e}^{-\left(\mu^0_D - \mu^0_N\right)/RT} \tag{4}$$

$$K^0_{obs} = \mathrm{e}^{-\left(\Delta G^0_{obs}\right)/RT} \tag{5}$$

At temperatures below t_m, $\Delta G^0_{obs} > 0$. Therefore, $\mu^0_D - \mu^0_N > 0, \mu^0_D = \Delta G^0_{obs} + \mu^0_N$. The values of ΔG^0_{obs} determined at 37˚C for both HSA_{99} and HSA_{96} are given as their ΔG^0_{37} values in **Table 1**.

In terms of the specific samples at hand, for HSA_{99},

$$\Delta G^0_{obs-99} = 11.9 \text{ kcal/mol} = \mu^0_{D-99} - \mu^0_{N-99} \tag{6}$$

Similarly for HSA_{96},

$$\Delta G^0_{obs-96} = 26.1 \text{ kcal/mol} = \mu^0_{D-96} - \mu^0_{N-96} \tag{7}$$

If the denatured state for both species is arbitrarily assigned as the reference state, $\mu^0_{D-99} = \mu^0_{D-96} = 0$, then $\mu^0_{N-99} = -\Delta G^0_{obs-99}$ and $\mu^0_{N-96} = -\Delta G^0_{obs-96}$. Henceforth for convenience we write $\mu^0_{N-99} \equiv \mu^0_{96}$ and $\mu^0_{N-96} \equiv \mu^0_{96}$.

The general treatment above requires slight modification to properly consider the HSA_{96} preparation which, as stated earlier and evidenced by **Figure 1**, is primarily comprised of two different populations of the protein, termed $HSA_{96\text{-}H}$ and $HSA_{96\text{-}L}$. To account for this mixture we write,

$$\mu^0_{96} = x_H \mu^0_{96-H} + \left(1 - x_H\right) \mu^0_{96-L} \tag{8}$$

with x_H equal to the mole fraction of $HSA_{96\text{-}H}$ in the HSA_{96} preparation. Here it is assumed if a small amount of HSA_{99} is present, it is so in a negligible amount (<5%). As such, writing Equation (8) in this manner ignores the slight presence of HSA_{99} (reckoned as the small inflection on the low temperature side of the HSA_{96} melting transition in **Figure 1**). Equation (8) assumes that other than $HSA_{96\text{-}H}$ the remaining protein is in the $HSA_{96\text{-}L}$ form.

As stated previously we assume $HSA_{96\text{-L}}$ and $HSA_{96\text{-H}}$ that comprise the HSA_{96} preparation are in many ways analogous to the defatted ($HSA_{L\text{-F}}$) and un-defatted ($HSA_{H\text{-F}}$) forms of HSA previously studied and reported [1] [15] [16]. Their different forms were observed under conditions very similar to ours (heating rate, buffer composition, protein concentration, relative fraction of FA). From their analysis they reported a value of x_H in Equation (8) around 0.3 [1] [16]. They also reported measured average values for the transition enthalpies for the $HSA_{L\text{-F}}$ and $HSA_{H\text{-F}}$ species. These were, $\Delta H_{L\text{-}F} = 4.18$ cal/g for the defatted species and $\Delta H_{H\text{-}F} = 5.16$ cal/g, for the un-defatted species [1]. The molecular weight of HSA (66,500 g/mol) provides $\Delta H_{L\text{-}F} = 280.06$ kcal/mol and $\Delta H_{H\text{-}F} = 345.72$ kcal/mol. Reported t_m values for $HSA_{L\text{-F}}$ and $HSA_{H\text{-F}}$ were 65.7˚C and 78.3˚C, respectively. These combined with $\Delta H_{L\text{-F}}$ and $\Delta H_{H\text{-F}}$ values provide an estimate on the transition entropies $\Delta S_{L\text{-}F}$ and $\Delta S_{H\text{-}F}$ for the reported defatted and un-defatted species. That is, $\Delta S_{L-F} = \dfrac{\Delta H_{L-F}}{T_{M-LF}} = \dfrac{280060}{338.85} = 826.5 \text{ cal/K} \cdot \text{mol}$ and $\Delta S_{H-F} = \dfrac{\Delta H_{H-F}}{T_{M-HF}} = \dfrac{345720}{351.45} = 983.7 \text{ cal/K} \cdot \text{mol}$. If these reported enthalpy and entropy values are assumed for the standard state, then estimates on the standard state free-energy at 37˚C, ΔG_{37}^0, of 23.9 kcal/mol and 39.6 kcal/mol were obtained for the $HSA_{L\text{-F}}$ and $HSA_{H\text{-F}}$ structures, respectively. In analogy with Equations (7) and (8) these ΔG_{37}^0 values yield the chemical potentials $\mu_{L-F}^0 = -23.9$ kcal/mol and $\mu_{H-F}^0 = -39.6$ kcal/mol for the defatted and un-defatted forms of HSA. The difference, $\mu_{L-F}^0 - \mu_{H-F}^0 = 16.5$ kcal/mol. In the discussion that follows it is arbitrarily assumed for the example shown that the values for $HSA_{96\text{-L}}$ and $HSA_{96\text{-H}}$ are approximately 75% of reported values for the presumably analogous forms, $HSA_{L\text{-F}}$ and $HSA_{H\text{-F}}$. That is we assume $\mu_{96-H}^0 = -33.8$ kcal/mol and $\mu_{96-L}^0 = -17.3$ kcal/mol, with the same *relative* difference $\mu_{96-L}^0 - \mu_{96-H}^0 = 16.5$ kcal/mol. This is probably not an unrealistic assumption based upon differences in data analysis and reported thermodynamic parameters compared to ours [1]. For both sets of values the *relative* difference remains the same.

With these assumptions, estimates on the value of x in our experiments can be made by rearranging Equation (8),

$$x_H = \frac{\left(\mu_{96}^0 - \mu_{96-L}^0\right)}{\left(\mu_{96-H}^0 - \mu_{96-L}^0\right)}$$

Using the values given above for $\mu_{96-H}^0 = -33.8$ and $\mu_{96-L}^0 = -17.3$ and the measured value of $\mu_{96}^0 = -26.1$ kcal/mol we find $x_H = 0.53$.

In a separate graphical analysis of the HSA_{96} thermogram (not shown), it was assumed the composite curve in **Figure 1** collected for the HSA_{96} sample was comprised of just two major components, $HSA_{96\text{-H}}$ and $HSA_{96\text{-L}}$. The graphical curve analysis returned an estimate of $x_H = 0.5$ which is in agreement with what was calculated assuming the values of μ_{96-H}^0 and μ_{96-L}^0 above, but about 20% larger than reported [16] for the relative fractions of the analogous forms $HSA_{L\text{-F}}$ and $HSA_{H\text{-F}}$. In the remaining development a value of $x_H = 0.53$ is assumed for the initial composition of HSA_{96}.

4.2. Attachment of Biotin to HSA

Consider the following cases. For the HSA_{99} preparation,

$$\text{HSA}_{99} + Bio - attach \rightarrow \text{HSA}_{99-Bio}$$

where $Bio - attach$ represents the generic attachment reaction that depends on the site of attachment, Bio = M or NS. Consider single site attachment first, *i.e.* Bio = M. In analogy with Equation (6) the observed standard state free-energy of the melting reaction for $HSA_{99\text{-M}}$ is given by,

$$\Delta G_{obs-99-M}^0 = \mu_{D-99-M}^0 - \mu_{N-99-M}^0 \tag{9}$$

Again, letting $\mu_{D-99-M}^0 = 0$ and $\mu_{N-99-M}^0 \equiv \mu_{99-M}^0 = -16.8$ kcal/mol, which is compared to $\mu_{99}^0 = -11.9$ kcal/mol. As a result, $\mu_{99}^0 - \mu_{99-M}^0 = -11.9 - (-16.8) = 4.9$ kcal/mol, and the attached biotin increases the chemical potential of the $HSA_{99\text{-M}(x:1)}$ structure compared to HSA_{99}. In the above we have used the average value of $\Delta G_{obs-99-M}^0 = -\mu_{99-M}^0 = 16.8$ kcal/mol evaluated from the average over the values obtained for

the $HSA_{99\text{-}M(x:1)}$ samples at x = 1, 3, and 10.

For the HSA_{96} preparation the thermogram is comprised of two overlapping transitions. The lower temperature transition seems most affected by attachment and is attributed to $HSA_{96\text{-}L}$ with biotin attached, *i.e.* $HSA_{96\text{-}L\text{-}M(x:1)}$, and assumed to be similar (but not identical) to $HSA_{99\text{-}M(x:1)}$

$$HSA_{96} + Bio - attach \rightarrow HSA_{96-L-Bio} + HSA_{96-H-Bio}$$

It is possible that during the attachment reaction some of the labeled $HSA_{96\text{-}H}$ molecules ($HSA_{96\text{-}H\text{-}M}$) convert to the $HSA_{96\text{-}L\text{-}M}$ form. To account for these considerations the measured chemical potential of the $HSA_{96\text{-}M}$ preparation is written as,

$$\mu^0_{96-M} = f_{96-H-M}\,\mu^0_{96-H-M} + \left(1 - f_{96-H-M}\right)\mu^0_{96-L-M} \tag{10}$$

Rearranging Equation (10) and solving for f_{96-H-M} provides an estimate on the fraction of $HSA_{96\text{-}H\text{-}M}$ molecules that remain following the attachment reaction, *i.e.*

$$f_{96-H-M} = \frac{\left(\mu^0_{96-M} - \mu^0_{96-L-M}\right)}{\left(\mu^0_{96-H-M} - \mu^0_{96-L-M}\right)}$$

We assume that biotinylation of HSA_{96-H-M} and HSA_{96-H-M} has the same effect as biotinylation of HSA_{99}, and similarly write the analogous chemical potentials, *i.e.*

$$\mu^0_{96-L-M} = \mu^0_{96-L} - 4.9 \text{ kcal/mol}$$

$$\mu^0_{96-L-M} = -17.3 - 4.9 = -22.2 \text{ kcal/mol}$$

and

$$\mu^0_{96-H-M} = \mu^0_{96-H} - 4.9 \text{ kcal/mol}$$

$$\mu^0_{96-H-M} = -33.8 - 4.9 = -38.7 \text{ kcal/mol}$$

And the average of the measured values of $\Delta G^0_{obs-96-M(x:1)}$ evaluated at x = 1, 3 and 10, corresponds to the chemical potential $\mu^0_{96-M} = -26.1$ kcal/mol. With the values of $\mu^0_{96-H-M} = -38.7$ kcal/mol, and $\mu^0_{96-L-M} = -22.2$ kcal/mol,

$$f_{96-H-M} = \frac{\left(\mu^0_{96-M} - \mu^0_{96-L-M}\right)}{\left(\mu^0_{96-H-M} - \mu^0_{96-L-M}\right)} = \frac{-26.1 - (-22.2)}{-38.7 - (-22.2)} = 0.24$$

This indicates that the fraction of molecules in the $HSA_{96\text{-}H\text{-}M}$ form decreases from 0.53 to 0.24 when the single site labeling reaction takes place. The result is approximately 50% of the $HSA_{96\text{-}H}$ in the original HSA_{96} preparation being converted in the single site attachment reactions.

Alternatively, consider the fraction of molecules f_{96-H-M} in the $HSA_{96\text{-}H\text{-}M}$ state (presumably now labeled) does not change during the attachment reaction, *i.e.* $f_{96-H-M} = 0.53$. How does the resulting value of μ^0_{96-H-M} change compared to μ^0_{96-H} due to the attachment reaction? Rearranging Equation (10) and solving for μ^0_{96-H-M},

$$\mu^0_{96-H-M} = \frac{\mu^0_{96} - \mu^0_{96-L-M}\left(1 - f_{96-H-M}\right)}{f_{96-H-M}} = \frac{-26.1 + 22.2(1 - 0.533)}{0.53} = -29.5 \text{ kcal/mol}$$

This is considerably smaller than $\mu^0_{96-H} = -38.7$ kcal/mol. So the effect of biotinylation on the HSA_{96} preparation is either to convert some fraction of the $HSA_{96\text{-}H\text{-}M}$ molecules to the $HSA_{96\text{-}L\text{-}M}$ form, or reduce the stability of $HSA_{96\text{-}H\text{-}M}$ compared to $HSA_{96\text{-}H}$.

Results of the above analysis and behavior of the measured thermograms are consistent with the following scenario. In the process of the attachment reaction a portion of the $HSA_{96\text{-}H}$ molecules get biotinylated and convert to $HSA_{96\text{-}L\text{-}M}$ essentially becoming $HSA_{99\text{-}M}$, which is much less stable than $HSA_{96\text{-}H}$ but more stable than HSA_{99} alone. Thus, there are two opposing effects of biotin attachment on protein stability. Biotin attachment to the $HSA_{96\text{-}L}$ and $HSA_{96\text{-}H}$ structures to create $HSA_{96\text{-}L\text{-}M}$ and $HSA_{96\text{-}H\text{-}M}$ increases their stabilities. But with the attachment reaction a fraction of the more stable, $HSA_{96\text{-}H}$ molecules are converted to the less stable $HSA_{96\text{-}L}$ form, then subsequently biotinylated to become $HSA_{96\text{-}L\text{-}M} \approx HSA_{99\text{-}M}$. In combination, the loss of a fraction of

the $HSA_{96\text{-H}}$ molecules through conversion results in a decrease in stability and reduces the chemical potential. This destabilization is overcome by attachment of biotin to $HSA_{96\text{-L}}$ to create $HSA_{96\text{-L-M}}$ resulting in an increase in chemical potential. This reduction and increase offset. As a consequence both the $HSA_{96\text{-M}}$ and HSA_{96} preparations have the same chemical potential.

Evidently, biotinylation increases stability of $HSA_{96\text{-L-M}}$ while reducing stability of $HSA_{96\text{-H-M}}$ compared to their unlabeled counterparts, $HSA_{96\text{-L}}$ and $HSA_{96\text{-H}}$, respectively. It is possible that binding of ligands that comprise the FA/G-LC contributes to enhanced stability of $HSA_{96\text{-H}}$ that must exist in a more stable conformation than $HSA_{96\text{-L}}$. $HSA_{96\text{-L}}$ may bind to the FA/G-LC ligands and have a structure and stability like HSA_{99} bound by the FA/G-LC ligands and have a different conformation than $HSA_{96\text{-H}}$. Clearly, the 3% contaminant, FA/G-LC, in the HSA_{96} preparation has quite a profound effect on the structure and stability of the different forms of HSA that comprise the HSA_{96} preparation.

For the case of multiple attachment, consider for the HSA_{99} preparation,

$$\mathrm{HSA}_{99} + Bio_{x:1} - attach \rightarrow \mathrm{HSA}_{99-Bio(x:1)}$$

where for multiple attachment Bio(x:1) = NS(x:1). For $HSA_{99\text{-NS}(x:1)}$,

$$\Delta G^0_{obs-99-NS(x:1)} = \mu^0_{D-99-NS(x:1)} - \mu^0_{N-99-NS(x:1)}$$

Again, letting $\mu^0_{D-99-NS(x:1)} = 0$, $\mu^0_{99-NS(x:1)} = -\Delta G^0_{obs-99-NS(x:1)}$. These values of ΔG^0_{37} are given in **Table 1**, and plotted versus attachment ratio, x, in **Figure 6**. Higher x results in increased stability of the $HSA_{99\text{-NS}(x:1)}$ structure compared to HSA_{99}. For the HSA_{99} preparation the effect of biotinylation is to incrementally increase ΔG^0_{37} (and t_m) with increased attachment ratio, x. These results for $HSA_{99\text{-NS}(x:1)}$ provide the basis for dissecting the effects of multiple attachment on the HSA_{96} preparation.

On the $HSA_{96\text{-NS}(x:1)}$ thermograms in **Figure 4** there is no sign of the high temperature transition attributed to the aforementioned $HSA_{96\text{-H}}$ structure. Apparently this would indicate an effect of the attachment reaction is conversion of *all* molecules to the $HSA_{96\text{-L-NS}(x:1)}$ type structure. Based on this observation, we assume the thermograms of the $HSA_{96\text{-NS}(x:1)}$ samples are comprised of contributions of the labeled $HSA_{96\text{-L-NS}(x:1)}$ which is similar, but not identical (especially at low attachment ratios) to $HSA_{99\text{-NS}(x:1)}$; and contributions from binding of the FA/G-LC to that structure, *i.e.* $\delta\mu^0_{96-FA-NS(x:1)}$. In this case the chemical potential for $HSA_{96\text{-NS}(x:1)}$ is written as,

$$\mu^0_{96-NS(x:1)} = \mu^0_{96-L-NS(x:1)} + \delta\mu^0_{96-FA-NS(x:1)}$$

or

$$\delta\mu^0_{96-FA-NS(x:1)} = \mu^0_{96-NS(x:1)} - \mu^0_{96-L-NS(x:1)} \tag{11}$$

If we assume in Equation (11) that $\mu^0_{96-L-NS(x:1)} = \mu^0_{99-NS(x:1)}$ then the observed differences, $\mu^0_{96-NS(x:1)} - \mu^0_{99-NS(x:1)} = \delta\mu^0_{96-FA-NS(x:1)}$ are the contributions of binding of the FA/G-LC to the chemical potential of $HSA_{96\text{-NS}(1:x)}$, a state believed to be HSA_{99} with attached biotin $\left(\mu^0_{96-L-NS(x:1)}\right)$ *and* bound by the FA/G-LC. Both biotinylation and FA/G-LC binding are stabilizing interactions.

Values of $\delta\mu^0_{96-FA-NS(x:1)} = \mu^0_{FA}$ are plotted versus attachment ratio (x) in **Figure 7**. As shown there, the value of $\delta\mu^0_{96-FA-NS(x:1)}$ is highest at the lowest attachment ratio where the contribution from FA/G-LC binding is greatest. As attachment ratio increases $\delta\mu^0_{FA-NS(x:1)}$ rapidly decreases to essentially zero at the higher biotinylation ratios. This decrease presumably corresponds to occlusion of FA/G-LC binding to $HSA_{96\text{-L-NS}(x:1)}$ by increased biotin attachment at the higher ratios. Given the above analysis and interpretation derived therefrom, we can provide an explanation of the apparently contrasting behaviors of the $HSA_{99\text{-NS}(1:x)}$ and $HSA_{96\text{-NS}(1:x)}$ species. Consider the following scenario for $HSA_{96\text{-NS}(1:x)}$. At the lowest attachment ratios, the protein resides as $HSA_{96\text{-L}}$ with biotin attached to a few sites and some FA/G-LC bound to other potential binding sites. This results in a structure with a stabilizing component in the biotin label (as indicated for $HSA_{99\text{-NS}(x:1)}$) and a further stabilizing component due to binding of FA/G-LC to $HSA_{96\text{-L-NS}(x:1)}$. As the attachment ratio increases more biotin is attached, displacing formerly bound FA/G-LC at new biotinylated attachment sites, and occluding further FA/G-LC-binding there. At higher levels of biotinylation, destabilization brought about by the loss of FA/G-LC binding is more than compensated for by the increase in stability afforded by the increased amount of attached biotin, resulting in a more stable structure with increased t_m and greater ΔG^0_{37} that approaches that of $HSA_{99\text{-NS}(x:1)}$ for $x > 20$. Thus, the behavior of $HSA_{96\text{-NS}(x:1)}$ can be summarized as follows. The attachment reaction results in conversion of the $HSA_{96\text{-H}}$ species to $HSA_{96\text{-L}}$. At the lowest attachment ratios ($x < 20$), the

$HSA_{96\text{-L-NS}(x:1)}$ structure is stabilized by FA/G-LC binding and attachment of biotin. At higher attachment ratios stability of the biotinylated structure increases, but FA/G-LC is released resulting in a conversion of the structure from $HSA_{96\text{-L-NS}(x:1)}$ to one more like $HSA_{99\text{-NS}(x:1)}$. If this is the case, the difference in the ΔG_{37}^{0} values for $HSA_{96\text{-NS}(x:1)}$ and $HSA_{99\text{-NS}(x:1)}$ in Equation (11), $\left(\mu_{96-NS(x:1)}^{0} - \mu_{99-NS(x:1)}^{0}\right) = \delta\mu_{96-FA-NS(x:1)}^{0} \approx 6.7$ kcal/mol at the lowest attachment ratio is a *direct* gauge of the added stabilization afforded by FA/G-LC binding to the $HSA_{96\text{-L}} \approx HSA_{99}$ structure.

4.3. Reversibility to HSA Thermograms

As mentioned previously, published melting studies of HSA reported observations, at temperatures approaching t_m, of a second reaction attributed to irreversible aggregation of the protein in the denaturation region [1] [12] [13] [15]. They noted the potential existence of a slow irreversible denaturation step(s) but concluded potential contributions to the overall measured thermogram were minimal. Irreversibility occurs due to intermolecular association of denatured HSA polypeptide strands. Such aggregation is not readily reversible in the transition region and can affect reversibility of the HSA melting transition [16]. Influence of irreversible denaturation on the primary melting transition of HSA can be minimized (somewhat) through appropriate choices of experimental parameters [12] [13] [16]. In effect, under optimally designed experimental conditions the temperature scanning rate is such that kinetics of the irreversible denaturation reaction are relatively much slower, and only begin to contribute significantly to the HSA melting transition at temperatures above the t_m. Since our experiments of HSA were carried out under similar conditions to those previously reported [1], it was assumed the measured HSA melting transitions are, for the most part, reversible. Inherent in the analyses that were performed was the choice of the "universal" reference state, *i.e.* the denatured state. Therefore, the possibility of heterogeneous denatured states, differing in character in addition to their ability to reversibly renature from the denatured state to the native state, is not considered.

Contributions of the irreversible transition to the measured ΔC_p values can also manifest in the thermogram baseline and therefore be reduced or subtracted out (somewhat) in the baseline analytical procedure. The irreversible reaction could also manifest in evaluated thermodynamic parameters of the melting transition, which assumes a truly equilibrium (reversible) process with parameters evaluated from the area under the baseline corrected thermogram. This process might influence absolute values of thermodynamic transition parameters, ΔH_{cal} and ΔS_{cal}, which may be lower (or higher) than what has been reported previously, depending on how much of the baseline encroaches on the melting of transition of HSA from the native to denatured form, and how much irreversibility affects the transition and choices made as part of the baseline analysis procedure. In our analysis as much as 30% of the total endotherm of HSA can be absorbed in the baseline. Our baseline analysis treatment was performed in a systematic fashion in precisely the same manner for all thermograms. Within the inherent

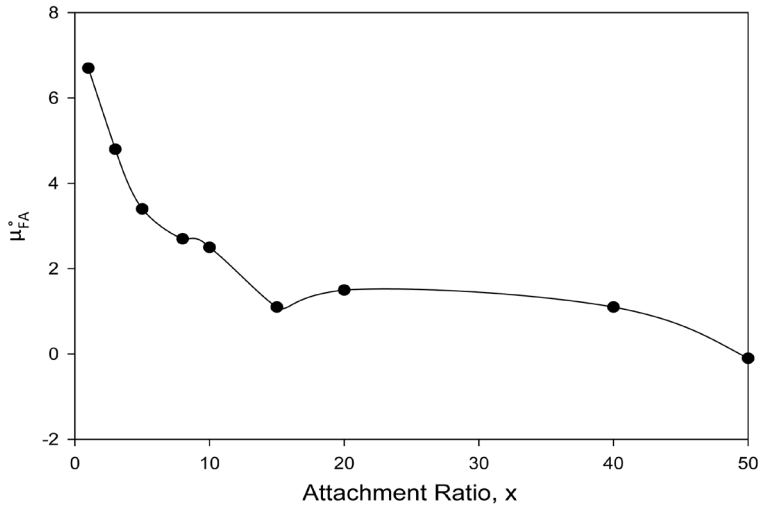

Figure 7. Values of the additional contribution to the chemical potential of HSA due to FA/G-LC binding, $\mu_{FA}^{0} = \delta\mu_{96-FA-NS(x:1)}^{0}$ (see text) plotted versus attachment ratio, *x*.

uncertainties underlying the operative analysis, *relative* values of the thermodynamic parameters are considered to be more quantitatively significant. Fortunately the analysis that was performed involved relative comparisons of the transition thermodynamic parameters.

5. Conclusion

In summary, results of this study have demonstrated that DSC is a sensitive method for monitoring solution conformation and stability of proteins (HSA). These experimental results and model analysis indicate that HSA can exist in very different thermodynamic states depending on the presence of a very small fraction (3%) of contaminants (likely) containing FA and globulin, termed FA/G-LC. These different states of HSA are also differentially affected by biotinylation. Thus, both biotinylation (adduct formation) and binding of ligands that comprise the FA/G-LC can stabilize the native form of HSA, and the different forms of HSA differentially respond to biotinylation in the presence or absence of FA/G-LC ligands.

Acknowledgements

This work was supported in part by grants IP-0912660 and IP-1026824 from the National Science Foundation. Portions of this work were also supported by a scholarship from the Ronald E. McNair Post-Baccalaureate Achievement Program awarded to Huyen Hoang. We thank Professor Jonathan B. Chaires and Dr. Nicola Garbett (University of Louisville) for helpful discussions and advice; and acknowledge Dr. Alan Ezrin (NX-PharmaGen) for suggesting these experiments. We thank Professor Todd Wimpfheimer (Salem State University) for helpful comments on the manuscript.

References

[1] Ross, P.D. and Shrake, A. (1988) Decrease in Stability of Human Albumin with Increase in Protein Concentration. *The Journal of Biological Chemistry*, **263**, 11196-11202.

[2] Peters, T. (1996) All about Albumin: Biochemistry, Genetics and Medical Applications. Academic Press, San Diego.

[3] Millán, F. and Mingo-Castel, A. (2003) A Chloroplast Transgenic Approach to Hyper-Express and Purify Human Serum Albumin: A Protein Highly Susceptible to Proteolytic Degradation. *Plant Biotechnology Journal*, **1**, 71-79. http://dx.doi.org/10.1046/j.1467-7652.2003.00008.x

[4] Sudlow, G., Birkett, D.J. and Wade, D.N. (1976) Further Characterization of Specific Drug Binding Sites on Human Serum Albumin. *Molecular Pharmacology*, **12**, 1052-1061.

[5] Fasano, M., Curry, S., Terreno, E., Galliano, M., Fanali, G., Narciso, P., Notari, S. and Ascenzi, P. (2005) The Extraordinary Ligand Binding Properties of Human Serum Albumin. *IUBMB Life*, **57**, 787-796. http://dx.doi.org/10.1080/15216540500404093

[6] Anderson, N.L. and Anderson, N.G. (1991) A Two-Dimensional Gel Database of Human Plasma Proteins. *Electrophoresis*, **12**, 883-906. http://dx.doi.org/10.1002/elps.1150121108

[7] Anderson, N.L., Polanski, M., Pieper, R., Gatlin, T., Tirumalai, R.S., Conrads, T.P., Veenstra, T.D., Adkins, J.N., Pounds, J.G., Fagan, R. and Lobley, A. (2004) The Human Plasma Proteome: A Nonredundant List Developed by Combination of Four Separate Sources. *Molecular & Cellular Proteomics*, **3**, 311-326. http://dx.doi.org/10.1074/mcp.M300127-MCP200

[8] Kragh-Hansen, U. (1981) Molecular Aspects of Ligand Binding to Serum Albumin. *Pharmacological Reviews*, **33**, 17-53.

[9] Rezaei-Tavirani, M., Moghaddamnia, S.H., Ranjbar, B., Amani, M. and Marashi, S.-A. (2006) Conformational Study of Human Serum Albumin in Pre-Denaturation Temperatures by Differential Scanning Calorimetry, Circular Dichroism and UV Spectroscopy. *Journal of Biochemistry and Molecular Biology*, **39**, 530-536. http://dx.doi.org/10.5483/BMBRep.2006.39.5.530

[10] Wetzel, R., Becker, M., Behlke, J., Billwitz, H., Böhm, S., Ebert, B., Hamann, H., Krumbiegel, J. and Lassmann, G. (1980) Temperature Behaviour of Human Serum Albumin. *European Journal of Biochemistry*, **104**, 469-478. http://dx.doi.org/10.1111/j.1432-1033.1980.tb04449.x

[11] Wallevik, K. (1973) Reversible Denaturation of Human Serum Albumin by pH, Temperature, and Guanidine Hydrochloride Followed by Optical Rotation. *Journal of Biological Chemistry*, **248**, 2650-2655.

[12] Pico, G.A. (1997) Thermodynamic Features of the Thermal Unfolding of Human Serum Albumin. *International Journal of Biological Macromolecules*, **20**, 63-73.

[13] Farruggia, B. and Pico, G.A. (1999) Thermodynamic Features of the Chemical and Thermal Denaturation of Human Serum Albumin. *International Journal of Biological Macromolecules*, **26**, 317-323. http://dx.doi.org/10.1016/S0141-8130(99)00054-9

[14] Farruggia, B., Rodriguez, F., Rigatuso, R., Fidelio, G. and Picó, G. (2001) The Participation of Human Serum Albumin Domains in Chemical and Thermal Unfolding. *Journal of Protein Chemistry*, **20**, 81-89. http://dx.doi.org/10.1023/A:1011000317042

[15] Shrake, A., Finlayson, J.S. and Ross, P.D. (1984) Thermal Stability of Human Albumin Measured by Differential Scanning Calorimetry. I. Effects of Caprylate and *N*-Acetyltryptophanate. *Vox Sanguinis*, **47**, 7-18. http://dx.doi.org/10.1111/j.1423-0410.1984.tb01556.x

[16] Shrake, A. and Ross, P.D. (1990) Ligand-Induced Biphasic Protein Denaturation. *Journal of Biological Chemistry*, **265**, 5055-5059.

[17] Michnik, A., Michalik, K., Kluczewska, A. and Drzazga, Z. (2006) Comparative DSC Study of Human and Bovine Serum Albumin. *Journal of Thermal Analysis and Calorimetry*, **84**, 113-117. http://dx.doi.org/10.1007/s10973-005-7170-1

[18] Michnik, A., Michalik, K. and Drzazga, Z. (2006) DSC Study of Human Serum Albumin Ageing Processes in Aqueous and Low Concentration Ethanol Solutions. *Polish Journal of Environmental Studies*, **15**, 81-83.

[19] Michnik, A. and Drzazga, Z. (2007) Effect of Ethanol on the Thermal Stability of Human Serum Albumin. *Journal of Thermal Analysis and Calorimetry*, **88**, 449-454. http://dx.doi.org/10.1007/s10973-006-8072-6

[20] Michnik, A. (2007) DSC Study of the Association of Ethanol with Human Serum Albumin. *Journal of Thermal Analysis and Calorimetry*, **87**, 91-96. http://dx.doi.org/10.1007/s10973-006-7825-6

[21] Meloun, B., Morávek, L. and Kostka, V. (1975) Complete Amino Acid Sequence of Human Serum Albumin. *FEBS Letters*, **58**, 134-137. http://dx.doi.org/10.1016/0014-5793(75)80242-0

[22] Dugaiczyk, A., Law, S.W. and Dennison, O.E. (1982) Nucleotide Sequence and the Encoded Amino Acids of Human Serum Albumin mRNA. *Proceedings of the National Academy of Sciences of the United States of America*, **79**, 71-75. http://dx.doi.org/10.1073/pnas.79.1.71

[23] He, X.M. and Carter, D.C. (1992) Atomic Structure and Chemistry of Human Serum Albumin. *Nature*, **358**, 209-215. http://dx.doi.org/10.1038/358209a0

[24] Carter, D.C. and Ho, J.X. (1994) Structure of Serum Albumin. *Advances in Protein Chemistry*, **45**, 153-203. http://dx.doi.org/10.1016/S0065-3233(08)60640-3

[25] Sugio, S., Kashima, A. and Mochizuki, S. (1999) Crystal Structure of Human Serum Albumin at 2.5 Å Resolution. *Protein Engineering*, **12**, 439-446. http://dx.doi.org/10.1093/protein/12.6.439

[26] Huang, B.X., Dass, C. and Kim, H.-Y. (2005) Probing Conformational Changes of Human Serum Albumin Due to Unsaturated Fatty Acid Binding by Chemical Cross-Linking and Mass Spectrometry. *Biochemical Journal*, **387**, 695-702. http://dx.doi.org/10.1042/BJ20041624

[27] Curry, S., Brick, P. and Franks, N.P. (1999) Fatty Acid Binding to Human Serum Albumin: New Insights from Crystallographic Studies. *Biochimica et Biophysica Acta* (*BBA*)*—Molecular and Cell Biology of Lipids*, **1441**, 131-140. http://dx.doi.org/10.1016/S1388-1981(99)00148-1

[28] Azim-Zadeh, O., Hillebrecht, A., Linne, U., Marahiel, M., Klebe, G., Lingelbach, K. and Nyalwidhe, J. (2007) Use of Biotin Derivatives to Probe Conformational Changes in Proteins. *Journal of Biological Chemistry*, **282**, 21609-21617. http://dx.doi.org/10.1074/jbc.M610921200

[29] Mock, D.M. and Lankford, G. (1990) Studies of the Reversible Binding of Biotin to Human Plasma. *Journal of Nutrition*, **120**, 375-381.

[30] Cohn, E.J., Strong, L.E., Hughes, W.L., Mulford, D.J., Ashworth, J.N., Melin, M. and Taylor, H.L. (1946) Preparation and Properties of Serum and Plasma Proteins. IV. A System for the Separation into Fractions of the Protein and Lipoprotein Components of Biological Tissues and Fluids 1a,b,c,d. *Journal of the American Chemical Society*, **68**, 459-475. http://dx.doi.org/10.1021/ja01207a034

[31] Quinlan, G.J., Martin, G.S. and Evans, T.W. (2005) Albumin: Biochemical Properties and Therapeutic Potential. *Hepatology*, **41**, 1211-1219. http://dx.doi.org/10.1002/hep.20720

[32] Oncley, J.L., Scatchard, G. and Brown, A. (1947) Physical-Chemical Characteristics of Certain of the Proteins of Normal Human Plasma. *Journal of Physical and Colloid Chemistry*, **51**, 184-198. http://dx.doi.org/10.1021/j150451a014

[33] Bruylants, G., Wouters, J. and Michaux, C. (2005) Differential Scanning Calorimetry in Life Science: Thermodynamics, Stability, Molecular Recognition and Application in Drug Design. *Current Medicinal Chemistry*, **12**, 2011-2020. http://dx.doi.org/10.2174/0929867054546564